Understanding the spectral and timing behaviour of a newly discovered transient X-ray pulsar Swift J0243.6+6124

Jaisawal, Gaurava K.; Naik, Sachindra; Chenevez, Jérôme

Published in:
Monthly Notices of the Royal Astronomical Society

Link to article, DOI:
10.1093/mnras/stx3082

Publication date:
2018

Document Version
Publisher's PDF, also known as Version of record

Monthly Notices of the ROYAL ASTRONOMICAL SOCIETY

MNRAS **474,** 4432–4437 (2018) doi:10.1093/mnras/stx3082
Advance Access publication 2017 December 5

Understanding the spectral and timing behaviour of a newly discovered transient X-ray pulsar Swift J0243.6+6124

Gaurava K. Jaisawal,[1]★ Sachindra Naik[2]★ and Jérôme Chenevez[1]★

[1]*National Space Institute, Technical University of Denmark, Elektrovej 327-328, DK-2800 Lyngby, Denmark*
[2]*Astronomy and Astrophysics Division, Physical Research Laboratory, Navrangapura, Ahmedabad - 380009, Gujarat, India*

Accepted 2017 November 22. Received 2017 November 20; in original form 2017 November 1

ABSTRACT

We present the results obtained from timing and spectral studies of the newly discovered accreting X-ray binary pulsar Swift J0243.6+6124 using *Nuclear Spectroscopy Telescope Array* observation in 2017 October at a flux level of ∼280 mCrab. Pulsations at 9.854 23(5) s were detected in the X-ray light curves of the pulsar. Pulse profiles of the pulsar were found to be strongly energy dependent. A broad profile at lower energies was found to evolve into a double-peaked profile in ≥ 30 keV. The 3–79 keV continuum spectrum of the pulsar was well described with a negative and positive exponential cutoff or high-energy cutoff power-law models modified with a hot blackbody at ∼3 keV. An iron emission line was also detected at 6.4 keV in the source spectrum. We did not find any signature of cyclotron absorption line in our study. Results obtained from phase-resolved and time-resolved spectroscopy are discussed in the paper.

Key words: stars: neutron – pulsars: individual: Swift J0243.6+6124 – X-rays: stars.

1 INTRODUCTION

Accretion-powered X-ray pulsars are among the brightest transient sources in the Galaxy. They were discovered in early seventies and are known to be powered by accretion of mass into the enormous gravitational field of the compact objects (see Paul & Naik 2011 for a review). Most of these transient pulsars belong to the class of high-mass X-ray binaries (HMXBs) in which a magnetized neutron star ($B \sim 10^{12}$ G) corotates with a supergiant or a Be-type optical companion around the common centre of mass. The strong field lines from the neutron star interact closely with the accreting plasma at the magnetospheric radius and channel the accreted matter on to the magnetic poles. This leads to the formation of hotspots or column-like structures at the magnetic poles of the neutron star which act as a source of immense high-energy radiations from the pulsars (Becker & Wolff 2007).

Depending on the nature of the optical companion, HMXBs can be broadly classified into (i) supergiant X-ray binaries and (ii) Be/X-ray binaries (Paul & Naik 2011; Reig 2011). In the first case, the neutron star orbits a supergiant companion of O or B spectral type and accretes matter from its dense stellar wind, while the compact object in Be/X-ray binaries is associated with a non-supergiant companion of B spectral type that shows emission lines in their optical and infrared spectra. These emission lines originated from a circumstellar decretion disc around Be stars (Reig 2011). The neutron star in these systems accretes matter while passing close to or through the circumstellar disc of the companion which results in strong X-ray outbursts. Be/X-ray binaries show normal (Type-I) or giant (Type-II) outbursts in which X-ray luminosity of pulsar gets enhanced by a factor of 10 or more. Type-I outbursts ($\sim 10^{37}$ erg s^{-1}) are periodic and coincide with the periastron passage, whereas Type-II outbursts ($\geq 10^{38}$ erg s^{-1}) are rare and do not show any orbital dependency (Reig 2011 and reference therein). The spin period of the neutron star in these systems ranges from a few seconds to 1000 s and is known to follow a positive correlation with orbital period in the Corbet diagram (Corbet 1986).

The new X-ray transient Swift J0243.6+6124 was discovered by *Swift* observatory on 3 October 2017 at a flux level of ∼80 mCrab (Kennea et al. 2017). The source was first thought to be a gamma-ray burst (GRB) or Galactic transient (Cenko et al. 2017). However, the increasing flux from continuous monitoring ruled out the possibility of a GRB. X-ray pulsations at ∼9.86 s were detected from the source using data from *Swift*/XRT and *Fermi*/GBM (Jenke & Wilson-Hodge 2017; Kennea et al. 2017). This confirmed the nature of Swift J0243.6+6124 as a pulsating neutron star (Bahramian, Kennea & Shaw 2017). Within the X-ray error box of the transient source, a B type star (USNO-B1.0 1514-0083050) was detected which is most likely the optical counterpart of the system (Kennea et al. 2017; Stanek et al. 2017; Yamanaka et al. 2017). Further monitoring of the companion showed a tentative presence of hydrogen and helium emission lines in the optical spectra, indicating the system to be a Be/X-ray binary (Kouroubatzakis et al. 2017). Using optical

★ E-mail: gaurava@space.dtu.dk (GKJ); snaik@prl.res.in (SN); jerome@space.dtu.dk (JC)

observations of the Be counterpart of the X-ray source, the distance of the system is reported to be 2.5 (Bikmaev et al. 2017) whereas data from Gamma-ray Burst Monitor (GBM) onboard *Fermi* obtained during the October 2017 X-ray outburst yielded the source distance of 4 kpc (Doroshenko, Tsygankov & Santangelo 2017). In this work, we have studied detailed spectral and timing properties of the pulsar for the first time by using *Nuclear Spectroscopy Telescope Array* (*NuSTAR*) observation during 2017 October outburst. A description about observation, results, and discussion is presented in Sections 2, 3, and 4 of the paper, respectively.

2 OBSERVATION AND ANALYSIS

Following the discovery of the transient source and its interesting X-ray activity, a Target of Opportunity (ToO) observation of Swift J0243.6+6124 was performed with *NuSTAR* on 2017 October 5 (Harrison et al. 2013). The observation was carried out for a total elapsed time of ∼37 ks with *NuSTAR* equivalent to an effective exposure of ∼14.3 ks (Obs-id: 90302319002). During the observation, the source was detected in the rising phase of the outburst at a flux level of ∼280 mCrab in 15–50 keV range with *Swift*/BAT.

The first hard X-ray focusing observatory, *NuSTAR*, was launched in 2012 June by NASA (Harrison et al. 2013). It covers soft to hard X-ray energy range from 3 to 79 keV with the help of two identical grazing angle focusing telescopes. The mirrors of these optics are coated with Pt/SiC and W/Si multilayers in order to reflect high energy photons below 79 ∼keV on CZT detectors at the two focal planes FPMA and FPMB. We have followed standard procedures to analyse the *NuSTAR* data using NUSTARDAS 1.6.0 software of HEASOFT (version 6.19). The unfiltered events were reprocessed first in our study by using NUPIPELINE together with the updated version of Calibration data base (CALDB; released on 2017 October 02) files. The cleaned events generated after the reprocessing were used further to extract science products such as light curves, spectra, response matrices, and effective area files with NUPRODUCT package. The source light curves and spectra were accumulated from both the detectors FPMA and FPMB by considering a circular region of 180 arcsec around the source centre. The background products were produced in a similar manner by selecting a region away from the source.

3 RESULTS

3.1 Timing analysis

Source and background light curves were extracted at a time resolution of 100 ms by following the methods as described above. We also applied barycentric correction on the background-subtracted light curves to incorporate the effect of Earth and satellite motion relative to the barycenter of the Solar system. The pulsation from the neutron star was searched in these light curves by using the *standard* χ^2-maximization technique (EFSEARCH task of FTOOLS). We detected X-ray pulsations at 9.854 23 (5) s in the 3–79 keV barycentric-corrected light curves from both the detectors. The distribution between the maximum chi-square and the trial pulsar period was fitted with a Gaussian function to estimate the value of pulse period and the error (1σ) associated with it. Power Density Spectrum (PDS; POWSPEC tool) was also generated to confirm the pulsations detected in the X-ray light curves of the pulsar. In the PDS (Fig. 1), apart from the fundamental frequency corresponding to the spin period of the pulsar, multiple harmonics were also observed. Therefore, the pulsation at 9.854 23 (5) s was confirmed as the spin period of the neutron star. Pulse profiles of the pulsar in 3–79 keV range were generated by folding the light curves from FPMA and FPMB detectors at the estimated spin period and are shown in the top panel of Fig. 2. Broadband pulse profile was found to be of complex shape. It included a minor peak (05–0.8 phase range) followed by the main feature at late phases (1.0–1.5 range) of the pulsar. To understand the energy evolution of these peaks and pulsar emission geometry, we have folded energy-resolved light curves in different bands and presented in Fig. 2.

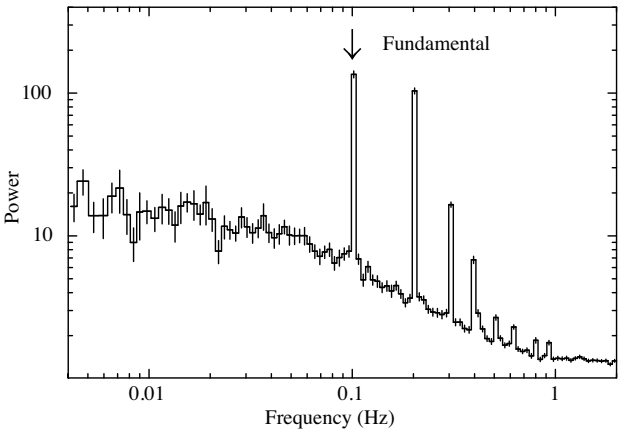

Figure 1. Power density spectra (PDS) of Swift J0243.6+6124 obtained from the FPMA data of *NuSTAR* observation on 2017 October 5. Pulsations at ∼9.85 s were clearly detected in PDS with its harmonics at higher frequencies. Arrow mark in the figure corresponds to the fundamental frequency of the pulsar in figure.

From this figure, it is clear that the pulse profiles are strongly energy dependent. A broad shape like profile seen at soft X-rays (3–7 keV) evolved into a double-peaked profile at hard X-rays ≥30 keV. Both the peaks were separated by approximately 180° phase. This suggests the viewing of both the poles of pulsar during observation. The energy evolution of the beam function can be traced successively in between low- and high-energy profiles. This evolution could also enlighten the broadening and phase shift in the minima of soft and hard X-ray pulse profiles (see Fig. 2). Pulsations were detected in light curves up to 79 keV. From the energy evolution, it is evident that emissions from both poles of the pulsar were contributing and shaping the pulse profiles during *NuSTAR* observation. To quantify the fraction of X-ray photons contributing to the observed pulsation, we estimated pulse fraction of the pulsar by using light curves in various energy ranges. The pulse fraction is defined as the ratio between the difference of maximum and minimum intensity to the sum of maximum and minimum intensity in the pulse profiles of the pulsar. Using the 3–79 keV light curve, the pulse fraction of the pulsar was estimated to be ∼28.8 ± 0.2 per cent. To investigate the change in pulse fraction with energy, we estimated pulse fraction in several energy ranges and presented in Fig. 3. The horizontal bars on data points in the figure represent the energy ranges in which pulse fraction has been estimated (see Fig. 2), whereas the vertical bars represent errors on the pulse fraction in a given energy range. The dotted line in the figure represents the value of pulse fraction of the pulsar in the entire 3–79 keV range. It can be seen that the pulse fraction of the pulsar increased towards high-energy ranges, indicating a large fraction of high-energy photons showing pulsating nature in the pulsar.

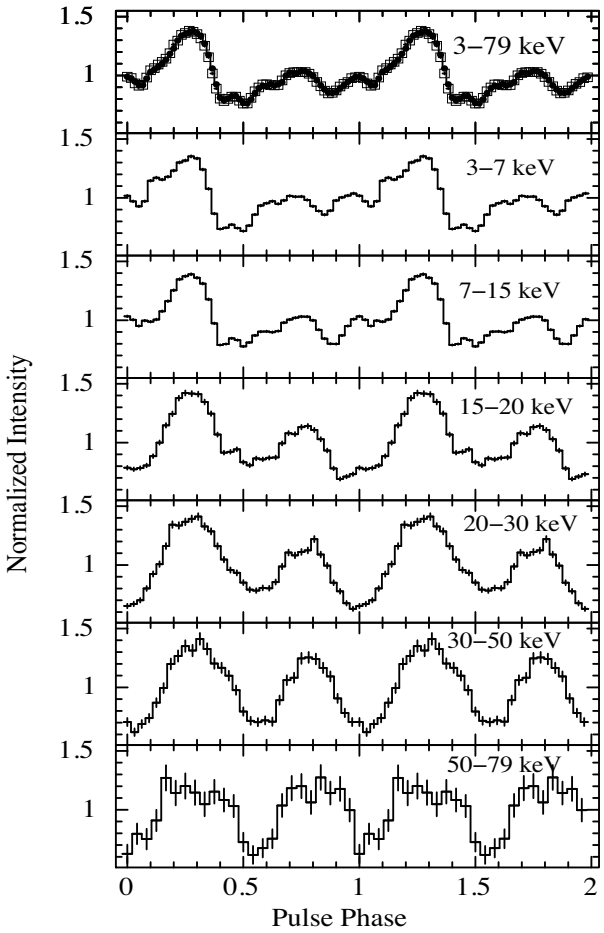

Figure 2. Pulse profiles of Swift J0243.6+6124 obtained from the background-subtracted light curves of FPMA and FPMB detectors of *NuSTAR* observation on 2017 October 5 are shown in the top panel. The data from FPMA and FPMB are consistent with each other and represented by solid dot and square in the panel, respectively. Energy-resolved pulse profiles of the pulsar from FPMA detector are also shown in the figure. These profiles are found to show strong energy dependence. A broad profile seen at soft X-rays evolved into a double-peaked profile at high energies. Pulsations were clearly detected in the light curves up to 79 keV. The error bars in each panel represent 1σ uncertainties. Two pulses in each panel are shown for clarity.

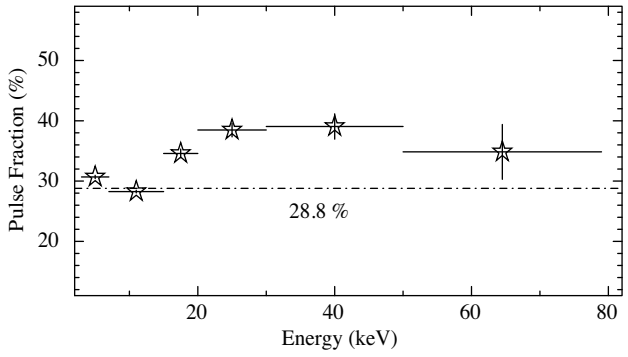

Figure 3. Pulse fraction variation of the pulsar with energy. The line is marked at the pulse fraction obtained from the pulse profile in 3–79 keV energy range.

3.2 Pulse-phase-averaged spectroscopy

To investigate the spectral properties of the pulsar Swift J0243.6+6124 and its emission components, phase-averaged spectroscopy was performed for the first time in 3–79 keV range by using data from *NuSTAR*. We have followed the procedure mentioned in Section 2 while extracting the spectral products. Source and background spectra obtained from both the detector units were grouped to achieve good signal-to-noise ratio, i.e. $\geq$128 counts per channel bins in our study. With appropriate response, effective area, and background files, broad-band spectral study was carried out with the data from FPMA and FPMB detectors of *NuSTAR* by using XSPEC package (ver. 12.9.0). All the spectral parameters for both detectors were tied during the fitting, while the relative normalizations of detectors were kept free. The cross-normalization between both detectors was consistent with suggested value by the instrumentation team.

The 3–79 keV energy spectrum of the pulsar was fitted with various traditional models such as power law modified with *Fermi*-Dirac cutoff power law (`fdcut`), power-law model modified with high-energy cutoff (HECut), cutoff power law (`Cutoff`), Negative and Positive exponential cutoff power law (NPEX), and `CompTT` models. Among these, NPEX is an empirical model which consists of two cutoff power-law models with negative and positive photon indices. While fitting the broad-band pulsar spectrum with this model, the photon index of the positive power law is fixed at 2, whereas the negative index is kept free. This model is developed by Makishima et al. (1999) and widely used to describe the broad-band spectrum of accretion-powered binary X-ray pulsars (e.g. Terada et al. 2007; Enoto et al. 2008; Naik et al. 2008, 2011 and references therein). A component for photoelectric absorption was also included in the expression. All the above models failed to explain the pulsar continuum and produced a poor fit with reduced-χ^2 of $\geq$2. However, the addition of a blackbody component (BBODYRAD in XSPEC) to these standard models yielded acceptable fits. We found that NPEX, HECut, and Cutoff models modified with a blackbody can well describe the energy spectra of the pulsar with reduced-χ^2 close to 1 in all three cases. A fluorescence emission line from iron was also detected at $\sim$6.4 keV in the spectra. Any signature of absorption-like feature or cyclotron absorption line was not seen in the 3–79 keV continuum. Spectral parameters obtained from all three models are given in Table 1. The value of absorption column density in the direction of the pulsar was found to be comparable to the value estimated from *Swift*/XRT data (Bahramian, Kennea & Shaw 2017; Kennea et al. 2017). Based on the spectral fitting and statistics, we consider NPEX and HECut models with a blackbody as best-fitting models. From the table, it can be seen that the blackbody temperature is relatively high, $\sim$3 keV in all the cases. This suggests a complex continuum of the pulsar during observation in 2017 October. We have shown broad-band energy spectrum fitted with two-component (NPEX and blackbody) model in Fig. 4. The second panel in the figure indicates corresponding spectral residuals. We have calculated the flux using the convoluted model `cflux` (available in XSPEC) in this paper.

3.3 Pulse-phase-resolved spectroscopy

Phase-resolved spectroscopy was performed to understand the emission geometry and surrounding of the pulsar for the first time in this paper using *NuSTAR* data. For this, we have accumulated the phase-sliced spectra in 16 phase bins using XSELECT package. The response matrices and effective area files as used for phase-averaged

Table 1. Best-fitting spectral parameters obtained from fitting the pulsar Swift J0243.6+6124 data from *NuSTAR* observation in 2017 October with high-energy cutoff power-law model, NPEX model, and exponential cutoff power-law model along with blackbody and Gaussian components. The error in spectral parameters is estimated for 90 per cent confidence interval.

Parameter	HECut+BB	NPEX+BB	Cutoff+BB
N_H[a]	0.9 ± 0.3	0.3 ± 0.2	0.6 ± 0.2
Photon index	1.25 ± 0.05	0.83 ± 0.06	1.10 ± 0.03
BB temp. (keV)	3.18 ± 0.04	3.01 ± 0.05	3.04 ± 0.03
BB norm.	1.6 ± 0.1	1.7 ± 0.1	2.04 ± 0.06
E_{cut} (keV)	7.0 ± 0.5	14.5 ± 2	24.5 ± 0.9
E_{fold} (keV)	27.8 ± 1.3	–	–
Fe line parameters			
Energy (keV)	6.41 ± 0.04	6.44 ± 0.04	6.45 ± 0.04
Width (keV)	0.26 ± 0.06	0.39 ± 0.06	0.45 ± 0.07
Eq. width (eV)	46 ± 7	71 ± 8	78 ± 9
Flux[b] (3–70 keV)	8.4 ± 0.1	8.4 ± 0.1	8.4 ± 0.1
Reduced-χ^2 (dofs)	1.06 (1573)	1.07 (1573)	1.11 (1574)

Notes.[a]Equivalent hydrogen column density (in 10^{22} atoms cm^{-2}).
[b]Absorption-corrected flux (in 10^{-9} erg cm^{-2} s^{-1}).

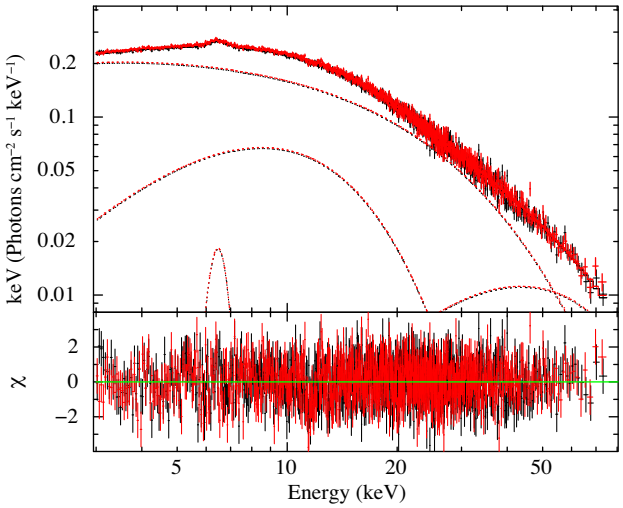

Figure 4. Energy spectrum of the pulsar Swift J0243.6+6124 in the 3–79 keV range obtained from FPMA and FPMB detectors of *NuSTAR* observation in 2017 October 5 along with one of the best-fitting model comprising a NPEX continuum with blackbody and an iron emission line. The bottom panel shows the contribution of the residuals to the best-fitting model.

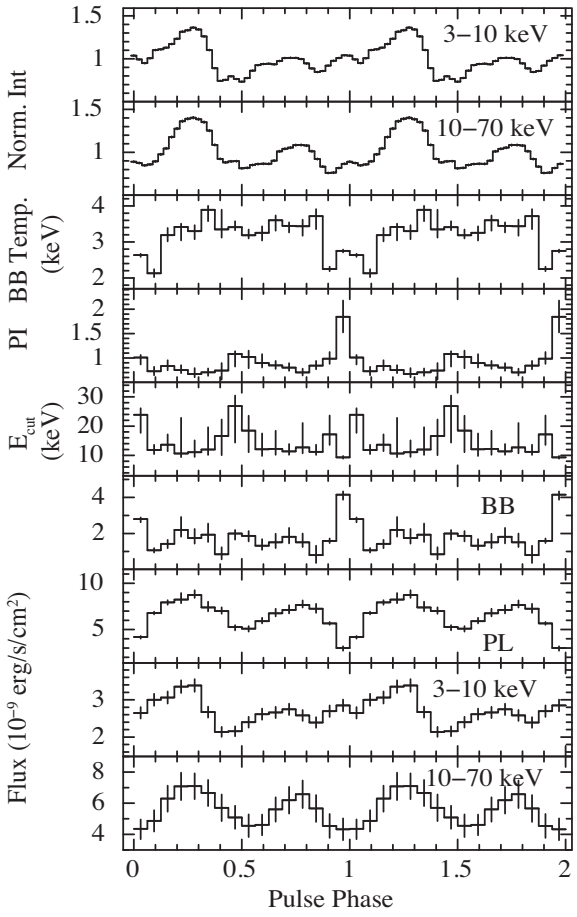

Figure 5. Spectral parameters (with 90 per cent errors) obtained from the phase-resolved spectroscopy of Swift J0243.6+6124 during *NuSTAR* observation with NPEX model along with blackbody component. Top and second panels show the pulse profile in the 3–10 and 10–70 keV energy ranges, respectively. The values of blackbody temperature, photon index, cutoff energy, blackbody flux, and power flux are shown in third, fourth, fifth, sixth, and seventh panels, respectively. The eighth and ninth panels represent the unabsorption source flux in 3–10 keV and 10–70 keV energy ranges, respectively.

spectroscopy were also considered in the phase-resolved spectroscopy. Spectral studies were carried out in the 3–70 keV energy range for each phase bins of the pulsar by using source and background spectra from FPMA and FPMB detectors along with corresponding response and effective area files. The best-fitting phase-averaged continuum such as NPEX and HECut models modified with a blackbody component was applied to describe the phase-resolved spectra. While fitting, the width of iron line was kept fixed at the respective value from Table 1.

Spectral parameters obtained from the phase-resolved spectroscopy are presented in Fig. 5 for NPEX with blackbody continuum model. The first and second panels of the figure show pulse profiles in 3–10 and 10–70 keV energy ranges, respectively. Corresponding source flux in these two bands is also given in bottom two panels (eighth and ninth) of the figure. Other spectral parameters such as blackbody temperature, photon index, and cutoff energy are shown in third, fourth, and fifth panels, respectively. All the parameters were varying significantly with pulse phase of the pulsar. Similar kind of variation in spectral parameters was also found with high-energy cutoff model with blackbody in our study. Therefore, we have only presented the results from phase-resolved spectroscopy with composite NPEX model. From this, the equivalent hydrogen column density (N_H) was found nearly constant throughout the pulse phases of the pulsar. However, the value of blackbody temperature was found to be high (above 3 keV) in 0.15 to 0.85 phase range (see the third panel in figure). Though the temperature at other phases is relatively low, a bump-like pattern was clearly evident in between 0.85 and 1.15 range of the profile. Corresponding to this phase range, blackbody flux was also estimated to be significantly high as compared to other phases of the pulsar (the sixth panel of the figure). Moreover, photon index was getting softer as well in this region. The cutoff energy was found to vary in between 10 and 30 keV with pulse phases. The power-law flux was showing a double peak-like pattern as in hard X-ray pulse profiles. The continuum fluxes (absorption-corrected) in 3–10 and

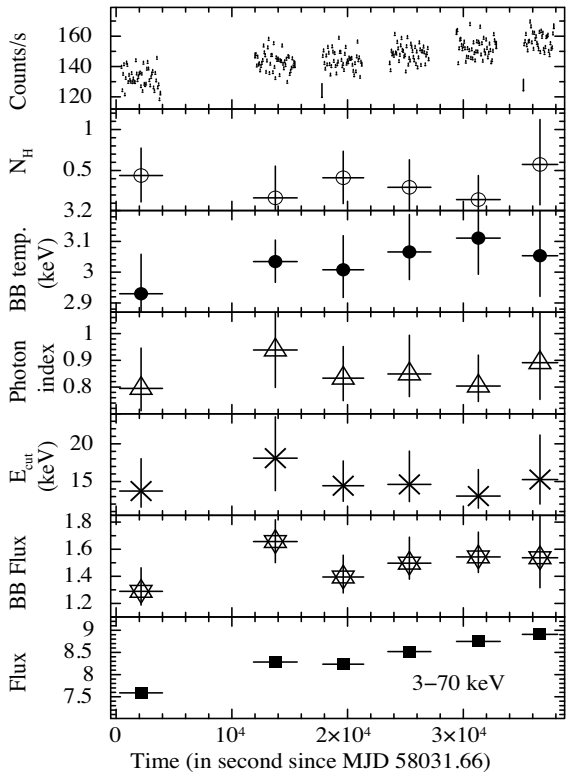

Figure 6. The parameters obtained from the time-resolved spectroscopy of the pulsar using NPEX with blackbody model during *NuSTAR* observation in 2017 October. The first panel shows the light curve in 3–79 keV. Variation in column density (in unit of 10^{22} cm^{-2}), blackbody temperature, photon index, cutoff energy, blackbody flux, and the source flux in 3–70 keV are shown in second, third, fourth, fifth, sixth, and seventh panels of the figure, respectively.

10–70 keV ranges were seen to follow the shape of pulse profiles in respective energy bands.

3.4 Time-resolved spectroscopy

During the *NuSTAR* observation, the source count rate was continuously increasing as seen from the light curve of the pulsar (Fig. 6). Therefore, time-resolved spectroscopy was performed to investigate the continuum evolution and changes in spectral parameters at different luminosity. Source light curve was divided in six small segments and the corresponding spectral products were generated by providing good time interval for each of them. We have used the NPEX model with blackbody component in the study that provided a best fit for spectra in the 3–79 keV range. The hardness ratio was also checked by dividing the light curve of 10–70 keV to 3–10 keV energy range. Any significant change in the ratio was not detected.

The parameters obtained from time-resolved spectroscopy are shown in Fig. 6 with the 3–79 keV light curve from FPMA detector of *NuSTAR* in the first panel. The values of column density (in unit of 10^{22} cm^{-2}), blackbody temperature, photon index, cutoff energy, blackbody flux, and the source flux (in 3–70 keV) are presented in second, third, fourth, fifth, sixth, and seventh panels of the figure, respectively. Most of these parameters were found to be moderately variable throughout the observation. An increasing trend in blackbody temperature was detected with luminosity. At the same time, the photon index appeared to be relatively soft. The value of source flux was found to increase by about 17 per cent at the end of the observation as compared to the first segment of light curve.

4 DISCUSSION AND CONCLUSIONS

We have studied spectral and timing characteristics of the newly discovered transient Swift J0243.6+6124 using data from *NuSTAR* in 2017 October. The detection of strong X-ray pulsations in our study confirms this source as a pulsar. During the observation, the source flux was detected to be 8.4×10^{-9} erg cm^{-2} s^{-1}. Assuming a typical distance of 2.5 kpc (Bikmaev et al. 2017), the pulsar luminosity can be calculated to be $\sim 6.5 \times 10^{36}$ erg s^{-1} in the 3–70 keV energy range. This is a classic luminosity at which neutron stars accrete above sub-critical regime or close to the critical luminosity depending on the magnetic field (Becker et al. 2012). It is believed that most of the emission from accretion-powered pulsars is due to Comptonization of seed photons in accretion column located on the surface (Becker & Wolff 2007). For sub-critical pulsars, the bulk Comptonization of only blackbody seed photons leads to high-energy radiations from the hotspot. A pencil beam pattern is expected from the pulsar in this regime. In case of bright (critical or super-critical) sources, thermal and bulk Comptonization of seed photons (blackbody, bremsstrahlung and cyclotron radiations) shape soft to hard X-ray emissions in the presence of radiative dominating shock in the column. Therefore, the beam function of these pulsars can be complicated or as a mixture of pencil or fan geometry in critical or super-critical luminosity regimes.

In the present study, pulse profiles were found to be strongly energy dependent. Most of the Be/X-ray binary pulsars show energy-dependent and complex pulse profiles. They also include multiple absorption dips at certain phases (Jaisawal, Naik & Epili 2016; Epili et al. 2017 and references therein). These dips are found strongly dependent on energy and are thought to originate from absorption by matter in the form of narrow strips that are phase-locked to the neutron star. We have not observed any strong dip or corresponding increase in the column density at pulse phases from phase-resolved spectroscopy of Swift J0243.6+6124 . Pulse profiles in our study were found to evolve from broad peak-like structure to a double-peaked profile at higher energies. The presence of a double-peaked profile suggests the emissions from both the poles during *NuSTAR* observation. Soft X-ray radiations from these hotspots probably originate in a form of fan beam pattern that produced broad peak-like profile in 3–7 keV whereas the hard X-rays were emitted from poles of the neutron star in pencil beam pattern. This can contribute to viewing of both the magnetic poles of neutron star and explain the origin of double-peaked profiles in hard X-rays.

Despite the complex physical mechanism for pulsar emission, the energy spectrum of these sources can be described with simple continuum models such as Cutoff, HECut, and NPEX models. In the case of Swift J0243.6+6124, the continuum from *NuSTAR* data was found to be described with NPEX or HECut model along with a hot blackbody at $\sim$3 keV. A blackbody component associated with a continuum model was also detected in other pulsars such as EXO 2030+375 (Reig & Coe 1999), RX J0440.9+4431 (Ferrigno et al. 2013), GX 304-1 (Rothschild et al. 2017), and GX 1+4 (Yoshida et al. 2017). Assuming a distance of 2.5 kpc, the size of blackbody emitting region was calculated to be $\approx$325 m. This value is relatively small and consistent with the typical size of accretion column. Therefore, we expect that blackbody component is the intrinsic part of the spectral continuum of the pulsar which is originated from the accretion column. The blackbody flux is found to be $\sim$17 per cent of the source intensity.

During the *NuSTAR* observation, the source flux was found to be increasing. We have performed time-resolved spectroscopy to explore spectral evolution and possible state changes in the pulsar. Our results showed that the continuum was evolving with luminosity and showing effect of mass accretion rate. Based on this, a transition between sub-critical to super-critical accretion regimes and corresponding spectral variation or changes in emission geometry can be probed by future observations at different luminosity.

Apart from time evolution, we also mapped the surrounding and spectral characteristics of pulsar at different pulse-phases using phase-resolved spectroscopy. These parameters were found to be significantly variable. We detected a hot blackbody around the pulsar in a wide pulse phase range. Though relatively lower blackbody temperature was detected at pulse phase close to 1, flux of the same component was found higher. Moreover, the photon index was also detected to be softer close to phase 1. This signifies that hard X-ray emissions from the pulsar are relatively lower at this phase. However, it is clear that the contribution from blackbody component in this phase range causes excess emission in the soft X-rays as seen in the 3–10 keV pulse profile.

Accretion-powered X-ray pulsars are expected to be highly magnetic with field strength of the order of 10^{12} G. The detection of cyclotron resonance scattering features can provide a direct measure of the magnetic field. We have not found any signature of absorption-like feature in the pulsar spectrum in the present study. Future observations at higher luminosity of the pulsar can lead to possible discovery of a cyclotron line(s) and constrain the magnetic field of the pulsar.

ACKNOWLEDGEMENTS

We sincerely thank the referee for his/her suggestions on the paper. The research leading to these results has received funding from the European Union's Seventh Framework Programme and Horizon 2020 Research and Innovation Programme under the Marie Skłodowska-Curie Actions grant no. 609405 (FP7) and 713683 (H2020; COFUNDPostdocDTU). The authors would like to thank all the *NuSTAR* team members for ToO observation. This research has made use of data obtained through HEASARC Online Service, provided by the NASA/GSFC, in support of NASA High Energy Astrophysics Programs. This work used the NuSTAR Data Analysis Software (NUSTARDAS) jointly developed by the ASI Science Data Center (ASDC, Italy) and the California Institute of Technology (USA).

REFERENCES

Bahramian A., Kennea J. A., Shaw A. W., 2017, Astron. Telegram, 10866, 1
Becker P. A., Wolff M. T., 2007, ApJ, 654, 435
Becker P. A. et al., 2012, A&A, 544, 123
Bikmaev I. et al., 2017, Astron. Telegram, 10968, 1
Cenko S. B. et al., 2017, GCN Circular, 21960, 1
Corbet R. H. D., 1986, MNRAS, 220, 1047
Doroshenko V., Tsygankov S., Santangelo A., 2017, A&A, preprint (arXiv:1710.10912)
Enoto T. et al., 2008, PASJ, 60, 57
Epili P., Naik S., Jaisawal G. K., Gupta S., 2017, MNRAS, 472, 3455
Ferrigno C., Farinelli R., Bozzo E., Pottschmidt K., Klochkov D., Kretschmar P., 2013, A&A, 553, 103
Harrison F. A. et al., 2013, ApJ, 770, 103
Jaisawal G. K., Naik S., Epili P., 2016, MNRAS, 457, 2749
Jenke P., Wilson-Hodge C. A., 2017, Astron. Telegram, 10812, 1
Kennea J. A., Lien A. Y., Krimm H. A., Cenko S. B., Siegel M. H., 2017, Astron. Telegram, 10809, 1
Kouroubatzakis K., Reig P., Andrews J. A. Zezas, 2017, Astron. Telegram, 10822, 1
Makishima K., Mihara T., Nagase F., Tanaka Y., 1999, ApJ, 525, 978
Naik S. et al., 2008, ApJ, 672, 516
Naik S., Paul B., Kachhara C., Vadawale S. V., 2011, MNRAS, 413, 241
Paul B., Naik S., 2011, BASI, 39, 429
Reig P., 2011, Ap&SS, 332, 1
Reig P., Coe M. J., 1999, MNRAS, 302, 700
Rothschild R. E. et al., 2017, MNRAS, 466, 2752
Stanek K. Z., Kochanek C. S., Thompson T. A., Shappee B. J., Holoien T. W.-S., Prieto J. L., Dong S., 2017, Astron. Telegram, 10811, 1
Terada Y. et al., 2007, AdSpR, 40, 1485
Yamanaka M., Uemura M., Nakaoka T., Kawahara N., Abe T., 2017, Astron. Telegram, 10815, 1
Yoshida Y., Kitamoto S., Suzuki H., Hoshino A., Naik S., Jaisawal G. K., 2017, ApJ, 838, 30

This paper has been typeset from a TEX/LATEX file prepared by the author.